CHEMISTRY
AN ASIAN JOURNAL
www.chemasianj.org

Accepted Article

Title: Selenadiazole derivatives inhibit angiogenesis-mediated human breast tumor growth through suppressing VEGFR2-mediated ERK and AKT signaling pathway

Authors: Haoqiang Lai, Xiaoyan Fu, Chengcheng Sang, Liyuan Hou, Pengju Feng, Xiaoling Li, and Tianfeng Chen

To be cited as: *Chem. Asian J.* 10.1002/asia.201800110

Link to VoR: http://dx.doi.org/10.1002/asia.201800110

A Journal of
ACES Asian Chemical Editorial Society

A sister journal of Angewandte Chemie and Chemistry – A European Journal

WILEY-VCH

10.1002/asia.201800110

WILEY-VCH

Selenadiazole derivatives inhibit angiogenesis-mediated human breast tumor growth through suppressing VEGFR2-mediated ERK and AKT signaling pathway

Haoqiang Lai [#,a], Xiaoyan Fu[#,a], Chengcheng Sang [a], Liyuan Hou,[a] Pengju Feng,[a] Xiaoling Li,[*b] and Tianfeng Chen[*a]

Abstract: Selenadiazole derivatives (SeDs) have been found to show promising application in chemo-/radiotherapy through activating various downstream signaling pathways. However, the functional role of SeDs on angiogenesis, which is pivotal for tumor progression and metastasis, has not been elucidated. In the present study, we have examined the antiangiogenic activities of SeDs and elucidated their underlying mechanisms. The results showed that the as-synthesized SeDs not only enhanced their anti-cancer activities against several human cancer cells, but also showed more potent inhibition on human umbilical vein endothelial cells (HUVECs). The *in vitro* results suggested that, SeDs, especially **1a**, dose-dependently inhibited vascular endothelial growth factor (VEGF)-induced cells migration, invasion and capillary-like structure formation of HUVECs *in vitro*. **1a** also significantly suppressed VEGF-induced angiogenesis in Matrigel plug assay in C57/BL6 mice assay via down-regulation of VEGF. Furthermore, we found that **1a** significantly inhibited MCF-7 human breast tumor growth in nude mice without severe systematic cytotoxicity. **1a** was more effective in inhibiting cells proliferation and induced much more pronounce apoptosis effect in endothelial cells than MCF-7 cells, which implying that endothelial cells might be the primary target of **1a**. Further mechanic studies on tumor growth inhibition effects and neovessel formation suppression demonstrated that **1a** inhibited cell viability of MCF-7 and HUVECs by induction of cell apoptosis, accompanying by PARP cleavage and caspases activation. Additionally, **1a**-induced antiangiogenesis effect was achieved by abolishing VEGF-VEGFR2-ERK/AKT signal axis and enhanced the apoptosis effect through triggering reactive oxygen species (ROS)-mediated DNA damage. Taken together, these results clearly demonstrate the antiangiogenic potency of SeDs and the underlying molecular mechanisms.

Introduction

Angiogenesis, as one of the critical hallmarks of cancers, has been recognized to be the essential process in sustaining tumour initiation, growth, progression and metastasis[1]. Angiogenesis is a tightly regulated process involving multiple factors, and comprehensively triggered by different stimulation signaling pathway[1c, 2]. Nowadays, several pro-angiogenic molecules and regulatory have been characterized. VEGF as one of the most important pro-angiogenic molecules stimulates endothelial cells proliferation, migration and formation of neovessels through interaction with VEGFR-2[3]. Upon activation, various downstream molecules in cascades such as Src kinase, AKT, ERK, STAT3 and FAK can be activated and than result in angiogenesis stimulating signaling amplification, which coordinately leading to neovascular formation[4]. Consequently, molecules involved in these cascades could be exploited as ideal targets in angiogenesis restriction therapy. Moreover, extensive evidences have supported that anti-angiogenesis therapy has become one of the most promising strategy in cancer treatments. In recent decades, many antiangiogenic agents have been identified as potent anticancer drugs, and some of them have been applied into clinic, including monoclonal antibodies, small molecule tyrosine kinase inhibitors and signal pathway molecules inhibitor. However, toxicities, substantial costs and some severe side effects successively occurred[5]. Therefore, searching novel antiangiogenic agents with high performance and low toxicity and more affordable agents are urgently needed.

Selenium (Se), as essential trace element for humans, has been disclosed to display critical regulation role in physiological and pathological conditions. Moreover, recent studies revealed that selenium also could be sued in cancer prevention and cancer treatments when combined with other anticancer agents or radiation[6]. In the past decades, different chemical forms and dose of selenium have been investigated as promising anticancer agent in cancer treatment applications[7]. Among them, organoselenium compounds exert fascinating application in chemoprevention and chemotherapy for their pharmacological potential and interesting chemical properties when compared to inorganic selenium compounds[8]. Moreover, MeSe, and Methylselenol exhibited as antiangiogenic agents in cancer chemoprevention through inducing HUVEC cells apoptosis and cell cycle perturbation, which indicated the potential application of organoselenium compounds as antiangiogenesis agents[9]. Recently selenadiazole derivatives (SeDs) have triggered intense research interest due to their excellent anticancer biological activities, such as benzo[c]-[1,2,5]selenadiazole[10]5-methylbenzo[c][1,2,5]selenadiazole[11]5-nitrobenzo[c]-[1,2,5]selenadiazole[12], 1,2,3-thiadiazole and 1,2,3-selenadiazole derivatives[13]. In our previous works, we have rational synthesized a series of SeDs by chemical modification. We found that SeDs exhibited as strongly apoptosis inducer in A375 cells and MCF-7 cells through inducing mitochondria dysfunction[14], SeDs potently sensitized X-ray induced cancer cells apoptosis through targeting TrxR[15], antagonize hyperglycemia-induceddrug resistance in HepG2 cells and inhibited bladder cancer cell proliferation through activated ROS-mediated pathway[16]. These results all indicate that selenadiazole should be a good activity group in pharmaceuticals designing. However, little information of SeDs in antiangiogenesis is available. Therefore, searching for

[a] Department of Chemistry, Jinan University, Guangzhou 510632, China.
[b] Institute of Food Safety and Nutrition, Jinan University, Guangzhou 510632, China, tlxlli@jnu.edu.cn.
* Department of Chemistry, Jinan University Guangzhou 510632 (China) E-mail: tchentf@jnu.edu.cn.
# Authors contributed equally to the work

effective and safety SeDs as angiogenesis antagonizer have kindled great interest.

In our previous studies, we found that introduction of electron donating group(–CH_3) was able to increase the complex lipophilicity and cellular uptake[15a, 17], however, the introduction of electron-withdrawing group (–NO_2) reduced these properties[15a]. Moreover, the introduction of electron donating group (-CH_3, -OCH_3, -OH) and electron-withdrawing group (-NO_2, -Cl) display important role in anticancer activity of selenadiazole derivatives. For instance, the introduction of a nitro group (–NO_2) into SeD significantly enhanced the anticancer activity of SeDs, however, SeDs exerted more potent anticancer activities after the introduction of -OCH_3 into the modifies selenadiazole (SeDs)[12, 16, 18]. These results all indicate the critical role of electron donating group and electron-withdrawing group, and selenadiazole should be a good activity group in pharmaceuticals designing. Consequently, in order to searching better solubility and stability of SeDs as angiogenesis inhibitors, other electron donating groups(-$N(CH_3)_2$, -NH_2, -$NHCOCH_3$ and -OH) were used for SeDs designing. The results showed that SeDs significantly inhibited VEGF-induced angiogenesis in vitro and in vivo. Furthermore, we found that the introduction of –CH_3 group into the complex (**1a**) significantly enhanced the anticancer efficacy of SeDs. **1a** dramatically decreased the tumor growth of MCF-7 xenografts without severe systematically cytotoxicity. The studies on the underlying molecular mechanisms in HUVECs and MCF-7 cells revealed that SeDs strongly inhibited the activation of VEGF and VEGFR-2 phosphorylation, which blocked the transmission of the mitogenic signal through Akt and ERK1/2 pathways. **1a** also found to dose and time-dependently trigger reactive oxygen species (ROS) generation and induced DNA damage. Additionally, we found that **1a** dose-dependent suppressed the proliferation of MCF-7 cells through triggering apoptosis by inducing DNA damage and upregulating p-ATM, p-ATR and pp53 expression. Taken together, this study clearly demonstrated that SeDs targeted VEGF-VEGFR2-ERK/AKT signaling pathway, which resulted in suppression of tumor growth and angiogenesis. These results clearly demonstrate the antiangiogenic potency of SeDs and the underlying molecular mechanisms.

Results and Discussion

Synthesis and anticancer efficacy of SeDs

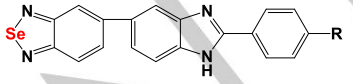

1a R=CH_3; **1b** R=Cl; **1c** R=H; **1d** R=OH;1e R=NO_2;
1f R=$N(CH_3)_2$; **1g** R=NH_2; **1h** R=$NHCOCH_3$

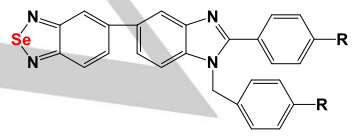

2a R=H; **2b** R=Cl; **2c** R=CH_3; **2d** R=OH

Figure 1. Chemical structure of **1a-1h** and **2a-2d**.

Table 1. Growth inhibitory effect of SeDs.

	Cell lines						
IC_{50} (μM)[a]	HUVEC	A375	A549	MCF-7	Hela	HepG2	HK-2[b]
1a	3.75±2.7	11.50±4.3	29.88±5.5	7.45±2.8	15.98±1.4	7.80±3.7	250.55±2.5
1b	112.85±2.7	139.79±3.6	77.93±2.6	139.10±4.1	51.20±8.6	7.60±4.5	>160
1c	208.04±9.3	355.7±1.4	168±3.8	79.20±7.8	176.50±4.9	305.80±7.1	>160
1d	53.07±1.5	59.19±3.6	26.8±1.4	93.98±9.5	30.98±7.2	7.55±8.2	99.26±4.3
1e	>160	>160	>160	>160	11.70±9.7	351.53±9.3	>160
1f	5.86±5.5	4.13±3.3	9.58±2.4	29.60±6.9	3.27±4.9	1.60±7.3	3.37±9.1
1g	78.13±3.4	118.17±4.1	16.87±3.3	68.90±7.2	40.20±5.2	129.25±4.8	154.49±1.5
1h	56.66±4.1	87.41±6.3	14.02±3.5	66.46±2.4	37.49±5.9	77.55±7.4	98.50±5.1
2a	310.76±3.6	278.56±5.8	246.73±8.5	253.34±1.5	39.23±1.2	333.36±1.3	>160
2b	149.26±2.5	279.40±5.5	199.70±1.1	216.36±6.6	139.39±1.2	246.69±5.9	277.67±8.8
2c	21.21±3.9	25.09±1.9	193.72±3.6	>160	25.38±7.4	70.64±11.2	176.73±9.1
2d	97.71±1.4	69.56±4.5	>160	70.37±4.8	45.90±1.8	42.69±13.2	75.68±3.6
Cisplatin	-	3.41-3.6	2.97-6.7	50.79±6.4	19.65±8.3	12.14±7.8	15.50±5.9

a. Cancer cells were exposed to different concentration of SeDs for 72 h and then cell viability was measured by MTT assay.
b. Normal cells.

Herein in this study, a series of phenylbenzo [1,2,5]selenadiazole derivatives were tested for their anticancer activities. First, in order to investigate the anticancer activities of these SeDs, we carried out MTT assay to evaluate the cytotoxicity of the SeDs on various cancer cells. As shown in **Table 1**, the complexes exhibited splendid broad-spectrum anticancer activity against series of human cancer cells, with **1a** exerted formidable inhibition effects in MCF-7 cells viability, as evidenced by the half maximal inhibitory concentration of **1a** is 7.45 μM, which is much lower than other cells. Intriguingly, we found that these SeDs also effectively suppressed endothelial cells proliferation. Furthermore, HUVECs seems to be more susceptible to these complexes when compared to the tested cancer cell lines, which indicated the potential antiangiogenesis capacity of these SeDs, especially for **1a**, 3.75 μM treatment of **1a** for 72 h was enough to cause more than half of HUVECs death. Meanwhile, we found that the synthesized analoguous O compound **3a** (**Figure S1-S4**) exhibited less potent inhibition effects towards HUVECs at the same concentration and the IC_{50} is 14.5 μM, which is much higher than **1a** (**Figure S15**). These results indicated that the Se burried in the compound makes special contributions to its antiangiogenesis activities. Moreover, we found that the as-synthesized complexes displayed less cytotoxicity to HK-2 human normal kidney cells, suggesting the specific cytotoxicity towards human cancer cells. Together, these results demonstrated the selective anticancer activities of organoselenium complexes, and the possible antiangiogenic activities of SeDs.

Organoselenium 1a inhibits tumor growth in *vivo*.

To evaluate the anticancer activities of organoselenium complexes, we selected **1a** for further evaluation through establishing a human breast tumor xenograft model in nude mice. After administrated with **1a**, we found that the tumor volume and tumor weight were dramatically inhibited when compared with the vehicle treatments (**Fig. 2A, B and 2C**). For instance, the tumor weight and tumor volume in the control group was about 1.45 ± 0.23 g and 2090 ± 0.12 mm^3, however, after treated with 2.5 and 5 mg/kg for 14 days, the tumor volume decreased to 1520 ± 0.22 mm^3 and 1370 ± 0.1 mm^3, and the tumor weight reduced to 0.98 ± 0.13 g and 0.62 ± 0.24 g respectively. Moreover, there is neglectable effect on the mouse

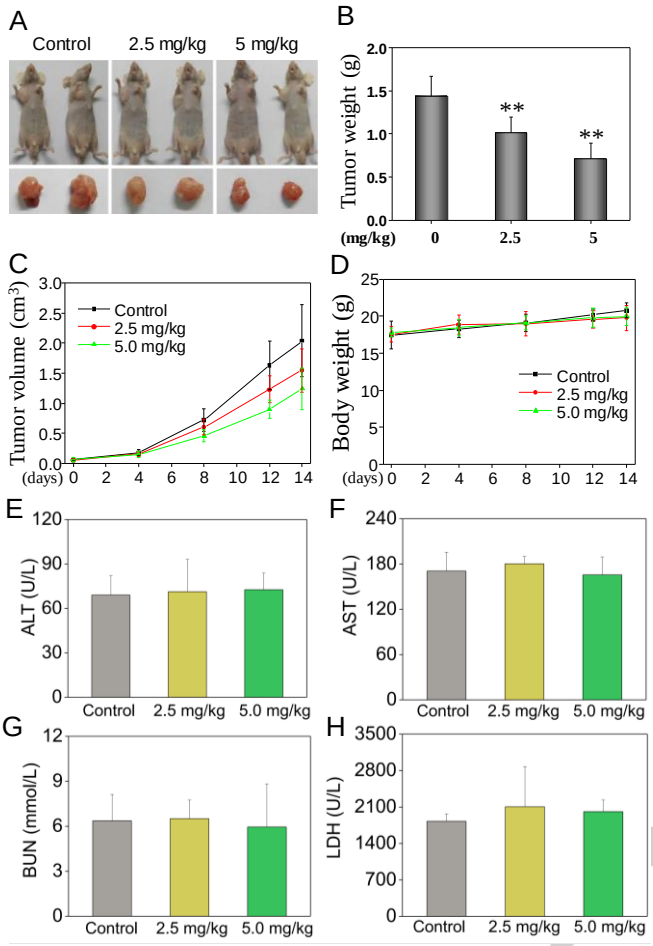

Figure 2. 1a induced MCF-7 tumor growth suppression *in vivo*. **1a** inhibited MCF-7 tumor growth as measured by tumor weight (A and B) and tumor volume (C) in MCF-7 xenografts models (D). (E-H) Hematological analysis of healthy and SeDs treatment mice (72 h). **P < 0.01 vs control.

body weight (**Fig. 2D**). In order to further evaluate the potential safety of **1a** *in vivo*, we conduct hematological analysis of **1a** as previously described[19]. Aspartate aminotransferase (AST) and alanine aminotransferase (ALT) are important indicators of liver function. blood ureannitrogen (BUN) and lactate dehydrogenase (LDH) are important indicators of kidney and heart function, respectively. The results of hematological analysis revealed that the mice treated with 2.5-5 mg/kg dose of **1a** showed no significant increased levels of AST, ALT, BUN, and LDH than the control group (**Figure 2E-2H**) as well as other evalution paramaters (**Figure S18**). Therefore, these results demonstrate that 2.5-5 mg/kg dose of **1a** might exerted slightly *in vivo* toxicity.Together, these data indicated that organoselenium **1a** had a potent therapeutic effect to suppress tumor growth *in vivo*, which is not attributed by its severe toxicity

Organoselenium 1a inhibits VEGF-induced cell migration, invasion and capillary structure formation of HUVECs *in vitro*.

Endothelial cell migration, invasion and tubular structure formation are all necessary steps for angiogenesis, tumor growth and tumor metastasis. Therefore, three well-established

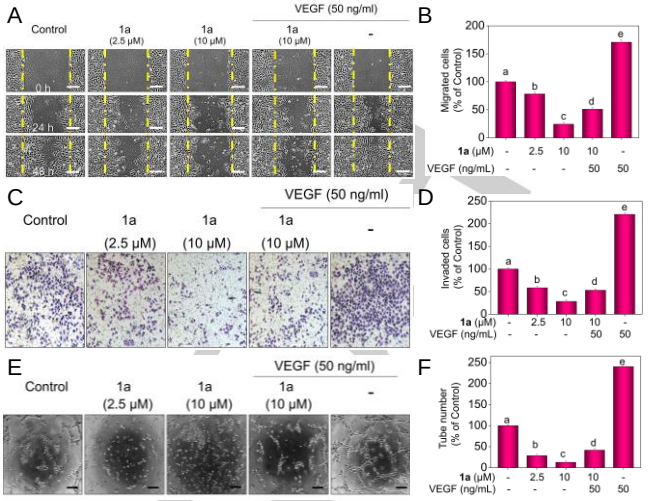

Figure 3. 1a inhibited VEGF-induced *in vitro* cell migration (A), invasion (C) and tube formation (E) in HUVECs. Quantitative analysis of migrated cells (B), invasived cells (D) and the length of tubular structure (F). Three independent experiments were carried out for these assays. The basal control groups were treated with 0.5% DMSO and 50 ng/mL of VEGF treatment was used as positive control group. Data in these experiments were expressed as means ± SD of triplicates. Bars with different characters (a-e) are statistically different at P<0.05 level. Scale bar: 100 nm.

models *in vitro* were employed to investigate the antiangiogeneiss activities of **1a**. Primarily, *in vitro* migration assay activities of **1a**. Primarily, *in vitro* migration assay was employed to detect the suppression effects of **1a** on HUVECs migration. As shown in **Figure 3A and 3B**, enhanced migration of HUVECs and complete wound closure by 48 h was observed in VEGF-treated group when comparing with the basal medium treatments. However, these effects were significantly inhibited by **1a** in a time- and dose- dependent manner, as convinced by the uncovered area. Moreover, **1a** (10 μM) dramatically suppressed the migrated effects of HUVECs stimulated by VEGF (50 ng/mL). Similarly suppression effects were also observed in the analoguous O compound **3a** treatments (**Figure S16**), but much less efficiency than **1a**.

Secondly, the effects of **1a** on HUVECs invasion were examined by transwell assay. As shown in **Fig.3C and 3D**,notable invasived cells in the control groups were observed in the lower side of transwell chamber after 24 treatments. VEGF treatment increased the invasived cells to the bottom of the chamber after 24 h treatment. However, **1a** dose-dependently restrained the cell invasion in a marginally manner, as evidenced by the decreased cell number. Similarly suppression effects were also observed in the co-treatment of **1a** (10 μM) and VEGF (50 ng/mL). The two models both demonstrated the potent inhibitory effect of **1a** on VEGF-induced HUVECs motility.

Two-dimensioned (2D) Matrigel assay was further used to detect the antiangiogenic effect of **1a** on HUVECs. As shown in **Figure 3E and 3F**, tubular structure was formed in the basal treatments and VEGF (50 ng/mL) stimulation. However, the structure was significantly destroyed after **1a** incubation for 8 h.

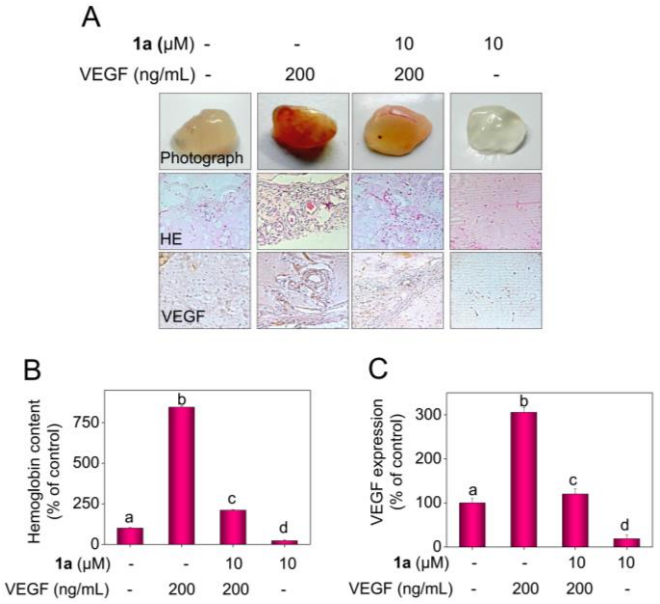

Figure 4. 1a restrained VEGF-induced new blood vessel formation *in vivo*. (A). Representive matrigel macroscopic appearance, HE staining and IHC of Matrigel plugs. Hemoglobin content (B) and VEGF expression (C) were employed to confirm the antiangiogenesis effect of **1a** *in vivo*. All data here are expressed as means±SD of triplicates. Bars with different characters (a-d) are statistically different at P<0.05 level.

Obvious antiangiogenic effects of **1a** on HUVECs *in vitro* was also observed in the co-incubation of VEGF (50 ng/mL) and **1a** (10 μM). These results indicate that **1a** displayed strongly antiangiogenic activities *in vitro*. Additionally, we found that **1a** and **3a** slightly inhibited the survival of endothelial cells during the treatments, which suggested that **1a** and **3a** inhibited VEGF-induced angiogenesis under non-toxic or subtoxic doses *in vitro*. (**Figure S17**).

Organoselenium 1a inhibits VEGF-induced angiogenesis *in vivo*.

To further evaluate the potential suppression effects of **1a** on angiogenesis *in vivo*, Matrigel plug assay was employed by using a C57BL/6 mice model. After 21-day administration, notable *in vivo* antiangiogenic effect of **1a** was observed. As shown in **Figure 4A** (**top**), when compared with the control groups, dark red matrigel plugs were obtained in VEGF (200 ng/mL) treatments, indicating the formation of a functional vasculature filled with intact red blood cells (RBCs). Histologic analysis of the Matrigel pellets using HE staining identified more and thicker erythrocyte-containing vesselsin group treated with VEGF alone than that of untreated group. In contrast, treatment of **1a** in combination with VEGF (200 ng/mL) potently inhibited angiogenesis *in vivo*, especially that 10 μM of **1a** treatment strongly inhibited the neovascularization in Matrigel plugs as evidenced by the pale color and a few infiltrating single cells (**Fig.4A, top and middle**). Quantification of angiogenesis by measuring hemoglobin content further confirmed the antiangiogenesis activities of **1a** (**Figure 4B**). Furthermore, VEGF as one of the most important pro-angiogenic molecules was also found to be significantly inhibited by **1a** as indicated by IHC assay (**Figure 4C**). Additionally, we found that **1a** exhibited strongly suppression effects in VEGF-induced neovascularization in CAM assay (**Figure S19**). These results clearly indicated that **1a** can inhibit VEGF-induced angiogenesis *in vivo*.

Organoselenium 1a induces apoptosis more effectively in HUVECs than that in MCF-7 cells.

Tumor growth depends on angiogenesis and the formation of new vessels requires angiogenic stimulation derived from tumor cells paracrine. However, whether the tumor suppression ccurs through affecting the endothelial cells function or cancer cells, or both was not ascertainable. To further characterize the molecular mechanism of growth inhibition in MCF-7 xenograft tumor induced by **1a**. We first examined the suppression effects of **1a** in HUVEC and MCF-7 cells. As illustrated in **Figure 5A and 5B**, **1a** inhibited HUVEC and MCF-7 cells proliferation in a dose-dependent manner. However, HUVECs were more susceptible to **1a** than MCF-7 cells, as indicated by the different cell viability suppression effects under the same concentration. We next characterized the antiproliferative molecular mechanism by using PI flow cytometry assay. As shown in **Figure 5C**, exposure of cells to **1a** resulted in a remarkable concentration-dependent elevation in the proportion of apoptotic cells in HUVECs, as can be seen in the increasing sub-G1

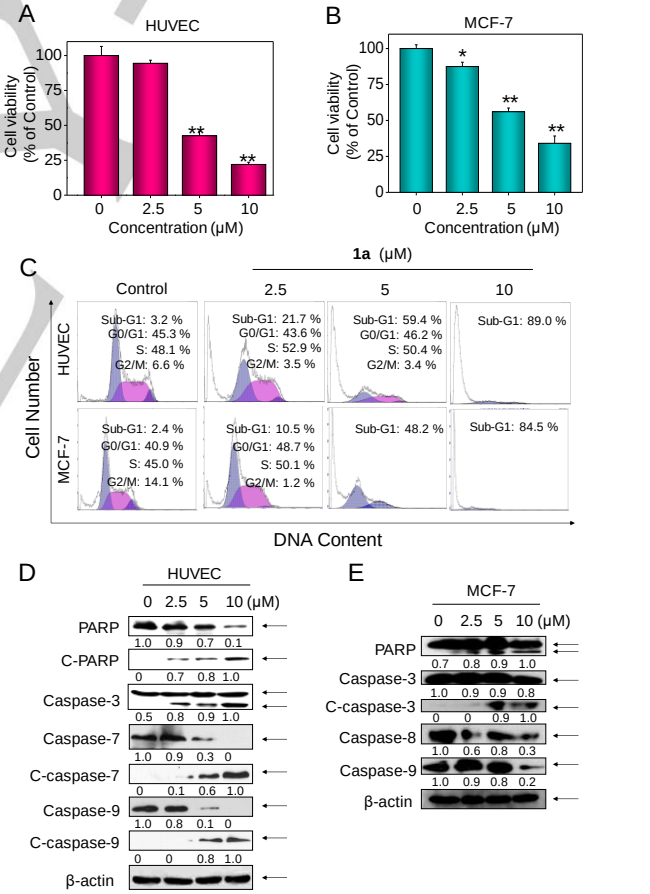

Figure 5. 1a inhibited cell viability of HUVEC and MCF-7 cells by induction of apoptosis. Cytotoxicity of **1a** towards HUVECs (A) and MCF-7 cells (B). C. **1a**-induced apoptosis in HUVEC and MCF-7 cells. **1a**-induced PARP cleavage and caspases activation in HUVEC (D) and MCF-7 cells (E). The proteins expression was examined by western blotting methods. All data were obtained from three independent experiments. *P < 0.05 vs untreated control. **P < 0.01 vs untreated control.

peaks from 3.2 % in control group to 21.7 %, 59.4 % and 89 % in **1a** treatments. Similarly, **1a** also induced concentration dependent apoptosis effect in MCF-7 cells, however, the apoptosis effect was less effective than HUVECs at the same concentration, suggesting the more potent apoptosis-inducing effects of **1a** in HUVECs, and the anti-angiogenesis mediated by **1a** on endothelial cells might be earlier than a direct cytotoxic effect on tumour cells. To further explore the underlying mechanism of apoptosis, fluorometric assay was conduct to investigate the caspases activation, which has been postulated to display essential role in apoptosis. Notably, **1a** treatment dramatically activated the caspase-3, caspase-9 and caspase-8 in HUVECs and MCF-7 cells (**Fig. S20**), indicating the activation of cell death mediated and mitochondria mediated apoptosis pathways. Moreover, activation of caspase-9, as thepredominant initiator in the mitochondria mediated apoptotic pathway, is more prominent than that of caspase-8 in HUVECs (**Fig. S20A**), which implys the mainly role of mitochondria-mediated apoptosis pathway induced by **1a**. Additionally, we found that **1a** triggered caspases activation was more formidable in HUVEC cells than in MCF-7cell, as can be seen in the different fluorescence intensity at the same dosage treatments. The apoptosis effects in HUVECs and MCF-7 cells induced by **1a** were further confirmed by western blotting assay (**Figure 5D and 5E**). For instance, **1a** treatment remarkably induced cleavage of PARP and caspases-3/-7/-8/-9. Taken together, these results all indicated that **1a** inhibited cell viability in HUVECs and MCF cells by induction of apoptosis and HUVECs were more sensitive to **1a** when compared to MCF-7cells.

Organoselenium 1a suppresses the VEGF-VEGFR2-ERK/AKT signaling axis.

Angiogenesis is strictly regulated by various angiogenesis stimulators and antiangiogenesis cytokines.VEGF, the most accepted pro-angiogenic growth factor, palys a critical role in regulating angiogenesis through binding to VEGF receptors (VEGFR1, 2 and 3)[20], and VEGFR2 is considered to exhibit the major role. After activation of VEGFR2, several downstream protein kinase pathways can be activated and thus modulated

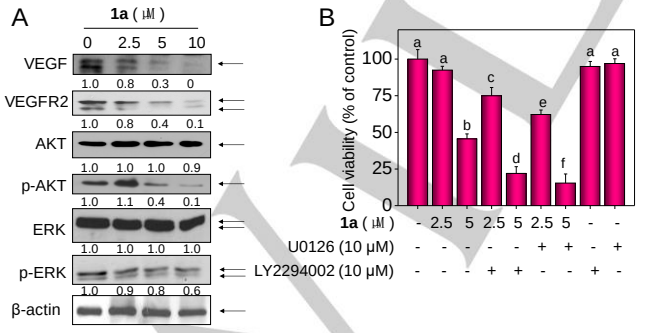

Figure 6. 1a suppresses VEGF–VEGFR2–ERK/AKT signaling axis. (A). **1a** inhibits the protein expression of VEGF, VEGFR2, ERK and AKT. (B). ERK and AKT inhibitor enhances **1a**-induced cell growth inhibition against HUVECs. Cells were pre-treated with 10 μM LY2294002 (Akt-upstream inhibitor) or 10 μM U0126 (ERK inhibitor) for 1 h and co-treated with **1a** for 72 h. Cell viability was detected by MTT assay. All data here are expressed as means±SD of triplicates. Bars with different characters are statistically different at P<0.05 level.

the angiogenesis procession. Such as, RAF/MEK/ERK and PI3K/AKT pathways are closely involved in endothelial cell proliferation, cell survival and angiogenesis[1c]. Abnormal activation of Raf/MEK/ERK and PI3K/Akt pathways often occurs in human cancer due to mutation or aberrant expression[21]. Therefore, cancer therapies of targeting components of this signal axis represent a promising tactic in recent years. To test the possibility of whether **1a**-induced inhibition of angiogenesis was associated with the suppression of VEGF-VEGFR2-ERK/AKT signalling axis, western blotting was employed to examine the changes of proteins in this axis. As shown in **Figure 6A**, treatment of HUVECs with **1a** dose-dependently decreased the protein expression of VEGF, VEGFR2, p-ERK and p-AKT. To further evaluate the role of ERK and AKT, the upstream inhibitor (U0126 and LY2294002) were used to examine **1a**-induced cell growth inhibition in HUVECs (**Figure 6B**). As illustrated in **Figure 6B**, enhancement of cell growth inhibition was observed in the pretreatment of LY2294002 and U0126, which indicated that **1a** induced anti-proliferation activity of HUVECs in ERK- and AKT-dependent manner. Taken together, these results indicated that VEGF/VEGFR2/AKT/ERK signaling pathway blockade was involved in **1a** antiangiogenesis activities.

Organoselenium 1a triggers DNA damage through ROS overproduction.

Triggering DNA damage has been postulated to be one of the most critical anticancer strategies in clinic. In response to DNA damage, cells may directly repaired DNA breaks or adducts as well as by halting cell cycle progression or triggering apoptosis. DNA damage results in autoactivation of ATM and ATR, which activates downstream substrates such as checkpoint kinase Chk1/Chk2, and H2AX and multi-functional transcription factor p53. P53 has been identified as a critical regulator in cell cycle progression and apoptosis through different mechanisms[22]. In our previous studies, SeDs are capable of inducing DNA damage through triggering ROS accumulation *in vitro*[12, 14a, 15b]. To examine whether **1a** induced DNA damage in HUVECs and MCF-7 cells, western blotting assay was exploited to detect the protein expression of p53 (Ser 15) and histone (Ser 139). As can be seen in **Figure 7A and S21**, there is an obvious elevation of p53 (Ser 15) and histone (Ser 139) protein expression in **1a** treatment, which indicated that **1a** induced DNA damage-mediate signaling pathway contributed to cells apoptosis and antiangiogenesis.

ROS has been considered to play an essential role in modulating apoptosis pathways[23]. Overproduction of ROS result in intracellular oxidative products accumulation, such as DNA strand breaks (DSBs). Increasing evidences demonstrate that ROS generation is involved in seleno complexes induce cell apoptosis[16, 24]. Therefore, DCFH-DA, a fluorescein-labeled probe, was used to detect **1a**-induced ROS accumulation. As shown in **Figure 7B**, treatment of HUVECs with indicated concentration of **1a** resulted in conspicuousness ROS accumulation in a time- and dose-dependent manner, which is further confirmed by the increasing fluorescence in **Figure S22**. Based on the importance of ROS, thiol-reducing antioxidants, glutathione (GSH), was introduced to examine the role of

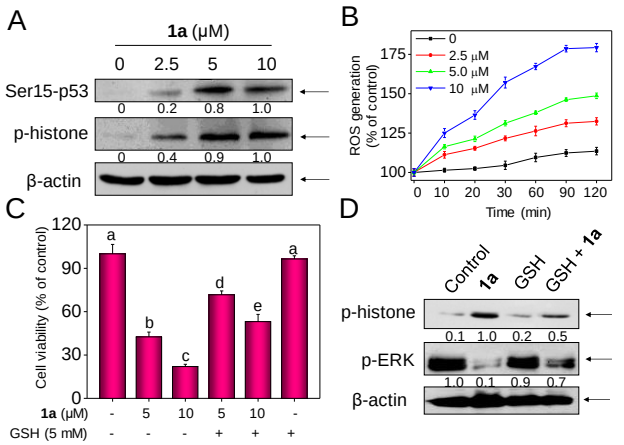

Figure 7. **1a** triggered DNA damage in HUVEC cells through ROS accumulation. (A). **1a**-induced DNA damage in HUVEC cells. (B). **1a** induced intracellular ROS generation in a time- and dose-dependent manner in HUVECs. (C). ROS scavengers prevents **1a**-induced cell growth inhibition. (D) DNA damage and ERK activation of HUVECs. All data here are expressed as means±SD of triplicates. All images shown here are representative of three independent experiments with similar results. Bars with different characters (a-e) are statistically different at P<0.05 level.

intracellular ROS in **1a**-induced apoptotic cell death. As shown in **Figure 7C**, pretreatment with 5 mM GSH for 2 h effectively protected HUVECs against **1a**-induced growth inhibition. The result indicated that **1a** inhibited HUVECs growth was depended on ROS generation. Furthermore, GSH addition significantly attenuated **1a**-induced DNA damage and ERK inactivation, indicating that ROS acts as upstream mediator of DAN damage and ERK pathway (**Figure 7D**). Taken together, these results demonstrated that **1a** inhibited angiogenesis-mediated human breast tumor growth by induction of HUVECs apoptosis through ROS-mediated DNA damage.

Conclusions

In this study, we have demonstrated the antiangiogenesis activities of SeDs. **1a** could effectively inhibit human breast tumor growth in xenograft mice through suppressing tumor angiogenesis by targeting VEGFR2 mediated AKT and ERK signaling pathway and then reinforced the apoptosis effect induced by **1a** through triggering DNA damage in endothelial cells. These results clearly demonstrate the antiangiogenic potency of SeDs and the underlying molecular mechanisms.

Experimental Section

Materials

VEGF was purchased from BD PharMingen (Bedford,MA). ECGM and M199 medium were purchased from Life Technologies, Invitrogen), Propidium iodide, DCF-DA, MTT, BCA kit for protein determination were purchased from Sigma. DMEM, FBS and penicillin-streptomycin were purchased from Invitrogen (Carlsbad, CA). Caspases substrate (Caspase-3/8/9), U0126 and LY2294002 were acquired from Calbiochem. All of the antibodies used in this study were purchased from Cell Signaling Technology (Beverly, MA). KoAc, 5-bromo-2-(4-methylphenyl) benzimidazole, NaH, DMF, $(BOC)_2O$, $PdCl_2$, andbis(pinacolato)diboron, 1,4-dioxane, $Pd(PPh_3)_4$ were obtained from sigma. All of the solvents used were of high-performance liquid chromatgraphy (HPLC) grade. SeDs were well solute in dimethyl sulphoxide (DMSO).The stock solution of SeDs were prepared in DMSO and kept at −20℃. SeDs were diluted in culture medium to obtain the desired concentration as needed.

Synthesis of selenadiazole derivatives

Generally, the **1a-1e** and **2a-2c** were synthesized as previously described[16, 24-25].

Synthesis of compound B

3 mmol [1,1'-biphenyl]-3,3',4,4'-tetraamine (**A**) was dissolved in 250 mL hydrochloric acid solution (HCl: H_2O = 1:5) in a 500 mL flask. Then 3 mmol SeO_2 which was dissolved in 20 mL hot distilled water was added into the flask drop by drop through a constant pressure funnel. The mixture was stirred for 2 h at r.t. After the 2 h, sodium hydroxide solution was used to change the pH to about 7.0, filtered, got the products, 4-(benzo[c][1,2,5]selenadiazol-5-yl)benzene-1,2-diamine (**B**). Yield: 90%.

General procedure for the synthesis of 1a-1f

1 mmol **B** dissolved in 25 mL DMF in a 50 mL flask. 1 mmol corresponding aromatic aldehyde was added into the flask with a catalyst, p-Methylbenzene sulfonic acid. The mixture stirred for 40 min at 80°C. After the reaction completed, the mixture was put into Na_2CO_3 (a.q.) stirring for 30 min, filtered to give the crude products, which was chromatographed over silica gel column (petroleum ether: ethyl acetate = 5:1) to afford pure compound **1a-1f**.

General procedure for the synthesis of 1g-1h

0.5 mmol **B**, 0.5 mmol 4-aminobenzoic acid and 10 g poly phosphoric acid (PPA) were added and mixed in DMSO (50 mL) homogeneously. The mixture was heated thrice at 20 % for 90 s; then the mixture was cooled down to room temperature, then water was added, crude product was filtered off and dried at room temperature. Solid product obtained by flash silicon column chromatography. （Petroleum ether : ethyl acetate = 20:1）.

General procedure for the synthesis of 2a-2d

1 mmol **B** dissolved in 25 mL DMF in a 50 mL flask. 2 mmol corresponding aromatic aldehyde was add into the flask with a catalyst, p-Methylbenzene sulfonic acid. The mixture stirred for 2 h at 80 °C. After the reaction completed, the mixture was put into Na_2CO_3 (a.q.) stirring for 30 min, filtered to give the crude products, which was chromatographed over silica gel column (petroleum ether: ethyl acetate = 7:1) to afford pure compound **2a-2d**.

Characterization of 1a-1h

ESI mass spectrometry was used to charecterized the final products of these complexes. **1a** Yield: 50 %; ESI-MS: m/z 391.1 $[M+H^+]^+$. **1b** Yield: 45 %; ESI-MS: m/z 409.4 $[M-H^+]^-$. **1c**: Yield: 40 %; ESI-MS: m/z 377.2 $[M+H^+]^+$. **1d**: Yield: 40 %; ESI-MS: m/z 393.3 $[M+H^+]^+$. **1e**: Yield: 47 %; ESI-MS: m/z 420.4 $[M-H^+]^-$.

1f: Yield: 38 %; ESI-MS: m/z 419.8291 $[M+H^+]^+$. Mp 331-332 °C. Elemental analysis calcd (%) for $C_{21}H_{17}N_5Se$: C, 60.29; H, 4.10; N, 16.74; found (%): C, 60.22; H, 4.05; N, 16.51. IR (KBr): v 750 (Se-N-Se), v 1365 (C-N) v 1610, 1550, 803 (C=C arom) cm^{-1}. ^{1}H-NMR: 400 MHz, DMSO-d^6, δ, ppm) 12.78-12.74 (d, 1H), 8.09-7.94(m, 5H), 7.94-7.85 (m, 1H), 7.71-7.57 (m, 2H), 6.87-6.85 (d, 2H), 3.01 (s, 6H) (**Figure S5-S6**).

1g: Yield: 43 %; TOF MS: m/z 392.0428 $[M+H^+]^+$. Mp 324-325 °C. Elemental analysis calcd (%) for $C_{19}H_{13}N_5Se$: C, 58.47; H, 3.36; N, 17.94; found (%): C, 58.42; H, 3.35; N, 17.91. IR (KBr): v 3419 (N-H), v 750 (Se-N-Se), v 1365 (C-N) v 1608, 1480, (C=C arom) cm^{-1}. ^{1}H-NMR: (400 MHz, DMSO-d^6, δ, ppm) δ 8.10 (s, 1H), 8.04 (m, 1H), 8.01 (d, 2H), 7.95-7.89 (t, 2H), 7.71-7.63 (m, 2H) , 6.72-6.69 (d, 2H). ^{13}C NMR (400 MHz, DMSO-d^6, δ): 160.75, 159.18, 153.52, 151.48, 141.75, 132.49, 130.45, 128.25, 123.23, 121.81, 118.99, 113.81. (**Figure S7-S9**).

1h: Yield: 35 %; TOF MS: m/z 434.0510 $[M+H^+]^+$. Mp 319-320 °C. Elemental analysis calcd (%) for $C_{19}H_{13}N_5Se$: C, 58.47; H, 3.36; N, 17.94; found (%): C, 58.42; H, 3.35; N, 17.91. IR (KBr): v 3427 (N-H), v 750 (Se-N-Se), v 1355 (C-N) v 1615, 1483, (C=C arom) cm^{-1}. ^{1}H-NMR: (400 MHz, DMSO-d^6, δ, ppm) 10.23 (s, 1H), 8.17-8.11 (t, 3H), 8.05-7.99 (m, 2H), 7.95 – 7.92 (m, 1H), 7.79 – 7.70 (m, 4H), 2.10 (s, 3H). ^{13}C NMR (400 MHz, DMSO-d^6, δ): 168.79, 160.51, 159.21, 141.08, 130.40, 129.73, 127.32, 126.71, 124.47, 123.23, 119.01, 118.84, 24.19 (**Figure S10-S12**).

Characterization of 2a-2d

2a: Yield: 31 %; ESI-MS: m/z 467.3 $[M+H^+]^+$. **2b:** Yield: 28 %; ESI-MS: m/z 535.4 $[M+H^+]^+$. **2c**: Yield: 25 %; ESI-MS: m/z 495.3 $[M+H^+]^+$.

2d: Yield: 30 %; ESI-MS: m/z 495.2 $[M-H^+]^-$. Mp 268-267 °C. Elemental analysis calcd (%) for $C_{26}H_{18}N_4O_2Se$: C, 62.78; H, 3.65; N, 11.26; found (%): C, 62.42; H, 2.61; N, 11.31. IR (KBr): v 748 (Se-N-Se), v 2965 (C-H), v 3920 (C-OH), v 1370 (C-N) v 1570, 1420, 814 (C=C arom) cm^{-1}. ^{1}H-NMR: (500 MHz, $CDCl_3$, δ, ppm) 8.11 (t, 2H), 8.02 (dd, 1H), 7.92 (d, 1H), 7.73 (dt, 2H), 7.54 (dd, 2H), 6.89 (dd, 4H) 6.79-6.59 (m, 2H) 5.56 (s, 1H), 5.47 (s, 1H) (**Figure S13-S14**).

Synthesis of compound 3a

5-(4,4,5,5-tetramethyl-1,3,2-dioxaborolan-2-yl)-2-(p-tolyl)-1H-benzo[d]imidazole (0.27 g, 0.81 mmol), 5-bromobenzo[c][1,2,5]oxadiazole (0.185 g, 0.93 mmol) and 25 mg $Pd(PPh_3)_4$ were dissolved in 1,4-dioxane (10 mL) under N_2 at rt.. After Na_2CO_3 (0.26 g, 2.45 mmol) being added to the mixure solution, the reaction was stirred for 16 h at 100 °C. The reaction was concentrated under vacuo and the residue was purified by alumina column chromatography with Ethyl acetate and Petroleum ether as eluants to give the title compound as a light yellow solid. Yield: 80 %. ESI-HRMS: m/z 327.12415 $[C_{20}H_{14}N_4O]+$. ^{1}HNMR (600 MHz, DMSO-d_6, δ): 13.07 (s, 1H), 8.30 (s, 1H), 8.14 (d, J = 28.2 Hz, 5H), 7.72 (s, 2H), 7.39 (d, J = 7.2 Hz, 2H), 2.40 (s, 3H). ^{13}CNMR (151 MHz, DMSO-d_6, δ): 150.18, 148.79, 145.10, 140.48, 134.56, 130.07, 127.60, 127.06, 116.85, 21.48.

Cell culture

Primary human umbilical vascular endothelial cells (HUVEC) were a kind gift from Dr. Liu (Guangzhou Jinan Biomedicine Research and Development Center, Guangdong Provincial Key Laboratory of Bioengineering Medicine, Jinan University, Guangzhou 510632, PR China). A375, A549, MCF-7, Hela, HepG2 and HK-2 were purchased from the American Type Culture Collection. HUVECs were cultivated in endothelial cell growth medium (ECGM):M199 medium (Life Technologies, Invitrogen) supplemented with 20% fetal bovine serum (FBS, Gibco) at 37℃ in a humidified (5% CO_2, 95% air) atmosphere. HK-2 and several human cancer cells (MCF-7, A375, $HepG_2$, A549 and Hela) were maintained in DMEM medium supplemented with 10 % FBS, 100 units/mL penicillin and 50 units/mL streptomycin at 37 ℃ in a humidified incubator with 5 % CO_2 atmosphere.

Tumor xenograft study

MCF-7 cells (about 1×10^6) in 100 μL serum-free medium were subcutaneously injected into the right oxter of male nude mice. After the average tumor volume reached about 50-70 mm^3 after 7 days, mice were randomly divided into 3 groups (8 mice/group) for control group, 2.5 mg/kg group and 5 mg/kg group (in this present study, we have carried out preliminary experiment to detect the LD_{50} (Lethal Dose, 50 %) of **1a** before the Tumor xenograft study. We found that the LD_{50} of **1a** was about 10 mg/kg, therefore, we choose 1/2 LD_{50} and 1/4 LD_{50} dosage of **1a** for the cancer treatment model.). Drugs were injected every other day, caudal vein, from the first day until the sixteenth day (8 times). At the termination of the experiments, tumors were harvested, photographed and weighed. Tumor dimensions were measured with calipers and the volume was calculated using the formula: volume = $l\times w^2/2$, with l being the maximal length and w being the width. All animal experiments were approved by the Animal Experimentation Ethics Committee.

Hematology Analysis

The mice were intravenous administration with **1a** at a dosage of 2.5 mg**/**kg and 5.0 mg/ kg of mouse body weight (n = 3, per group) and then sacrificed at 72 h.Then the the blood sample (72 h) was used for hematology analysis at Guangzhou Overseas Chinese Hospital.

Measurement of cytotoxicity

Cytotoxicity of organoselenium towards HUVECs, HK-2 and human cancer cell lines was measured as previously described[26]. Briefly, cells at a density of 2×10^3 per well were

allowed to grow for 24 h and then treated with different concentrations of complexes for 72 h. After that cell viability was measured by MTT assay. Cell viability in the presence of GSH or NAC (with powerful reducing capacity) was measured by trypan blue staining as previously reported[27]. The cell viability was expressed as % of control (as 100 %). The control groups were treated with 0.5 % DMSO.

Cell cycle distribution assay

Flow cytometric assay was exploited to detect the cell cycle distribution after **1a** incubation for the indicated times[28]. Briefly, **1a** treated cells were harvested and stained with PI after fixed with 70 % ethanol at -20 ℃ overnight, and the cell cycle distribution of the labeled cells were analyzed by Flow cytometer. The proportion of sub-G1 peaks were used to represent as apoptosis cells.

***In vitro* antiangiogenesis assay**

1a inhibited HUVECs migration, invasion and structure tube formation were measured as previously described[29].

Matrigel plug assay

The effect of **1a** treatment on *in vivo* angiogenesis was done by Matrigel plug assay as previously described[28].

Chorioallantoic membrane assay

Effect of **1a** on the new blood formation *ex vivo* was determined by CAM assay as previously described[15a].

Measurement of ROS generation

Effects of **1a** on intracellular ROS generation were evaluated by DCF fluorescence assay. The ROS level was detected in 2 h on a Tecan SAFIRE fluorescence reader, with the excitation wavelength at 488 nm and emission wavelength at 525 nm, respectively. Unlabeled cells in PBS were used as background control. Relative DCF fluorescence intensity of treated cells was expressed as percentage of control (as 100%).

Caspase activity assay

Activation of caspases in HUVECs or MCF-7 cells exposed to was examined by measuring the activities of caspase-3, -8, -9 using specific substrates (Ac-DEVD-AMC for caspase-3, Ac-IETD-AMC for caspase-8 and Ac-LEHD-AMC for caspase-9) as previously described[15a].

Western blot analysis

The effects of **1a** on the expression levels of proteins associated with different signaling pathways were examined by western blotting analysis as previously described[30].

Statistical analysis

Experiments were carried out at least in triplicate and repeated three times. All data were expressed as mean ± S.D. Statistical analysis was performed using SPSS statistical package (SPSS 13.0 for Windows; SPSS, Inc. Chicago, IL).

Acknowledgements

This work was supported by National High-level personnel of special support program (W02070191), YangFan Innovative & Entepreneurial Research Team Project (201312H05), Fundamental Research Funds for the Central Universities, National Key Scientific Instrument and Equipment Development Project. 2017YFF0104904 and Natural Science Foundation of Guangdong Province (2017A030313091).

Keywords: Selenadiazole • Anticancer •VEGF • Apoptosis • ROS

References:

[1] a) D. F. Quail, J. A. Joyce, *Nat Med* **2013**, *19*, 1423-1437; b) S. Valastyan, R. A. Weinberg, *Cell* **2011**, *147*, 275-292; c) P. Carmeliet, R. K. Jain, *Nature* **2011**, *473*, 298-307; d) G. Zerbini, M. Lorenzi, A. Palini, *New Engl J Med* **2008**, *359*, 763-763.

[2] S. M. Weis, D. A. Cheresh, *Nat Med* **2011**, *17*, 1359-1370.

[3] a) P. Saharinen, L. Eklund, K. Pulkki, P. Bono, K. Alitalo, *Trends Mol Med* **2011**, *17*, 347-362; b) M. Kowanetz, N. Ferrara, *Clin Cancer Res* **2006**, *12*, 5018-5022.

[4] a) E. J. Gordon, D. Fukuhara, S. Westrom, N. Padhan, E. O. Sjostrom, L. van Meeteren, L. He, F. Orsenigo, E. Dejana, K. Bentley, A. Spurkland, L. Claesson-Welsh, *Sci Signal* **2016**, *9*; b) J. Chen, J. Wang, L. Lin, L. He, Y. Wu, L. Zhang, Z. Yi, Y. Chen, X. Pang, M. Liu, *Mol Cancer Ther* **2012**, *11*, 277-287.

[5] a) B. Sennino, D. M. McDonald, *Nat Rev Cancer* **2012**, *12*, 699-709; b) L. G. Paz-Ares, B. Biesma, D. Heigener, J. von Pawel, T. Eisen, J. Bennouna, L. Zhang, M. Liao, Y. Sun, S. Gans, K. Syrigos, E. Le Marie, M. Gottfried, J. Vansteenkiste, V. Alberola, U. P. Strauss, E. Montegriffo, T. J. Ong, A. Santoro, *J Clin Oncol* **2012**, *30*, 3084-3092; c) V. Ranpura, S. Hapani, S. Wu, *J Am Med Assoc* **2011**, *305*, 487-494.

[6] a) H. Steinbrenner, B. Speckmann, H. Sies, *Antioxid Redox Sign* **2013**, *19*, 181-191; b) G. N. Schrauzer, *Crit Rev Biotechnol* **2009**, *29*, 10-17.

[7] a) Y. Huang, L. He, W. Liu, C. Fan, W. Zheng, Y.-S. Wong, T. Chen, *Biomaterials* **2013**, *34*, 7106-7116; b) W. Liu, X. Li, Y.-S. Wong, W. Zheng, Y. Zhang, W. Cao, T. Chen, *Acs Nano* **2012**, *6*, 6578-6591; c) T. Chen, Y.-S. Wong, W. Zheng, *Phytochemistry* **2006**, *67*, 2424-2430.

[8] a) A. P. Fernandes, V. Gandin, *Bba-Gen Subjects* **2015**, *1850*, 1642-1660; b) Y. Zhang, S. Zheng, J.-S. Zheng, K.-H. Wong, Z. Huang, S.-M. Ngai, W. Zheng, Y.-S. Wong, T. Chen, *Mol Pharmaceut* **2014**, *11*, 1282-1293; c) J. Su, H. Lai, J. Chen, L. Li, Y.-S. Wong, T. Chen, X. Li, *Plos One* **2013**, *8*; d) C. Liu, Z. Liu, M. Li, X. Li, Y.-S. Wong, S.-M. Ngai, W. Zheng, Y. Zhang, T. Chen, *Plos One* **2013**, *8*; e) M. Freitas, V. Alves, A. B. Sarmento-Ribeiro, A. Mota-Pinto, *Biochem Bioph Res Co* **2011**, *408*, 713-719.

[9] a) X. Wu, Y. Zhang, Z. Pei, S. Chen, X. Yang, Y. Chen, D. Lin, R. Z. Ma, *Bmc Cancer* **2012**, *12*; b) S. Chintala, T. Najrana, K. Toth, S. Cao, F. A. Durrani, R. Pili, Y. M. Rustum, *Bmc Cancer* **2012**, *12*; c) C. Jiang, K. H. Kim, Z. S. Wang, J. Lu, *Nutr Cancer* **2004**, *49*, 174-183.

[10] D. Plano, E. Moreno, M. Font, I. Encio, J. Antonio Palop, C. Sanmartin, *Arch Pharm* **2010**, *343*, 680-691.

[11] W. Wang, L. Li, S. Liu, C. Ma, S. Zhang, *J Am Chem Soc* **2008**, *130*, 10846.

[12] L. He, S. Ji, H. Lai, T. Chen, *J Mater Chem B* **2015**, *3*, 8383-8393.

[13] N. M. Mhaidat, M. Al-Smadi, F. Al-Momani, K. H. Alzoubi, I. Mansi, Q. Al-Balas, *Drug Des Dev Ther* **2015**, *9*, 3645-3652.

[14] a) Y. Luo, X. Li, X. Huang, Y.-S. Wong, T. Chen, Y. Zhang, W. Zheng, *Chem Pharm Bull* **2011**, *59*, 1227-1232; b) T. Chen, W. Zheng, Y.-S. Wong, F. Yang, *Biomed Pharmacother* **2008**, *62*, 77-84.

[15] a) H. Lai, Z. Zhao, L. Li, W. Zheng, T. Chen, *Metallomics* **2015**, *7*, 439-447; b) Q. Xie, Y. Zhou, G. Lan, L. Yang, W. Zheng, Y. Liang, T. Chen, *Biochem Bioph Res Co* **2014**, *449*, 88-93.

[16] Y. Liu, Y. Luo, X. Li, W. Zheng, T. Chen, *Chem-Asian J* **2015**, *10*, 642-652.

[17] J. Chen, Z. Luo, Z. Zhao, L. Xie, W. Zheng, T. Chen, *Biomaterials* **2015**, *71*, 168-177.
[18] Y. Yang, S. Deng, Q. Zeng, W. Hu, T. Chen, *Dalton T* **2016**, *45*, 18465-18475.
[19] N. Wang, Y. Feng, L. Zeng, Z. Zhao, T. Chen, *Acs Appl Mater inter* **2015**, *7*, 14933-14945.
[20] U. Harjes, *Nat Rev Cancer* **2017**, *17*, 708.
[21] R. K. Jain, P. Carmeliet, *Cell* **2012**, *149*, 1408-1408.e1401.
[22] Y. Chang, L. He, Z. Li, L. Zeng, Z. Song, P. Li, L. Chan, Y. You, X.-F. Yu, P. K. Chu, *ACS nano* **2017**, *11*, 4848-4858.
[23] T. Liu, L. Lai, Z. Song, T. Chen, *Adv Funct Mater* **2016**, *26*, 7775-7790.
[24] L. He, T. Chen, Y. You, H. Hu, W. Zheng, W.-L. Kwong, T. Zou, C.-M. Che, *Angew Chem Int Edit* **2014**, *53*, 12532-12536.
[25] W. Cao, X. Li, S. Zheng, W. Zheng, Y.-s. Wong, T. Chen, *Oncotarget* **2014**, *5*, 7431-7445.
[26] J. Su, H. Lai, J. Chen, L. Li, Y.-S. Wong, T. Chen, X. Li, *PLoS One* **2013**, *8*, e63502.
[27] C. Fan, W. Zheng, X. Fu, X. Li, Y. Wong, T. Chen, *Cell Death Dis* **2014**, *5*, e1191.
[28] X. Fu, Y. Yang, X. Li, H. Lai, Y. Huang, L. He, W. Zheng, T. Chen, *Nanamed-Nanotechnol* **2016**, *12*, 1627-1639.
[29] H. Lai, X. Zhang, P. Feng, L. Xie, J. Chen, T. *Chem-Asian J* **2017**, *12*, 982-987.
[30] Z. Song, Y. Chang, H. Xie, X.-F. Yu, P. K. Chu, T. Chen, *Npg Asia Mater* **2017**, *9*, e439.

10.1002/asia.201800110

WILEY-VCH

FULL PAPER

Herein we demonstrate that the introduction of $–CH_3$ group into SeDs (**1a**) potently inhibits MCF-7 tumor growth in nude mice without severe systematic cytotoxicity through suppressing tumor angiogenesis. Further mechanistic studies indicate that **1a**-induced antiangiogenesis effect was achieved by abolishing VEGF-VEGFR2-ERK/AKT signal axis and enhanced the apoptosis effect through triggering ROS-mediated DNA damage.

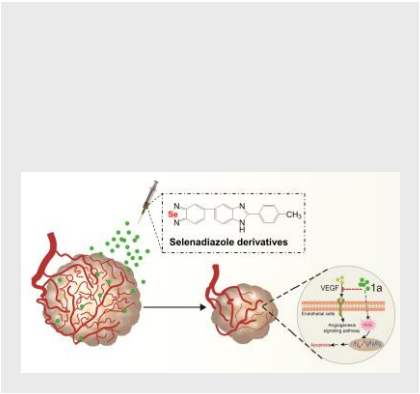

*Haoqiang Lai [#,a], Xiaoyan Fu[#,a], Chengcheng Sang,[a] Liyuan Hou,[a] Pengju Feng,[a] Xiaoling Li,[*b] and Tianfeng Chen[*a]*

Page No. – Page No.

Title